

Asymmetric Regularized CCA and Hierarchical Kernel Sentence Embedding for Image & Text Retrieval

Youssef Mroueh, Etienne Marcheret, Vaibhava Goel

IBM Watson Multimodal Group

mroueh,etiennem,vgoel@us.ibm.com

Abstract

Joint modeling of language and vision has been drawing increasing interest. A multimodal data representation allowing for bidirectional retrieval of images by sentences and vice versa is a key aspect. In this paper we present three contributions in canonical correlation analysis (CCA) based multimodal retrieval. Firstly, we show that an asymmetric weighting of the canonical weights, while achieving a cross-view mapping from the search to the query space, improves the retrieval performance. Secondly, we devise a computationally efficient model selection, crucial to generalization and stability, in the framework of the Björk Golub algorithm for regularized CCA via spectral filtering. Finally, we introduce a Hierarchical Kernel Sentence Embedding (HKSE) that approximates Kernel CCA for a special similarity kernel between distribution of words embedded in a vector space. State of the art results are obtained on MSCOCO and Flickr benchmarks when these three techniques are used in conjunction.

1. Introduction: Multimodal Retrieval

Modeling jointly language and vision has attracted a lot of attention recently. Generative models such as deep recurrent networks for the language modeling, in conjunction with deep convolutional neural networks on the image side have shown remarkable success in the task of image captioning [1, 2, 3]. Image and Text retrieval has been the focus of many recent works [4, 5, 6, 7]. The main contributions of this paper are :

1) *Mapping search items to the query space, AW-CCA.* In multimodal retrieval it is more common to embed the search space and the query space into a shared space (CCA in [5]) or to map the query item to the search space (cross-view mapping in [8]). In this paper we empirically show that mapping the search items to the query space outperforms those standard methods. We further show that this cross-view mapping from the search to the query space can be implemented

by a simple asymmetric weighting of the canonical correlation weights (AW-CCA), where the canonical weights of the search space are weighted by the canonical correlations.

2.a) *Regularization and Spectral Filtering for CCA.* Regularization is a key factor for the numerical stability as well as the generalization properties of a learning algorithm. We revisit Regularized CCA [9] within the framework of spectral filtering and the Björk Golub Algorithm [10] (Algorithm 1 in Appendix C). We present our regularized CCA within two spectral filtering regularization families: Tikhonov regularization [9] and truncated SVD (T-SVD) regularization [11]. T-SVD regularization is new in the CCA context.

2.b) *Fast T-SVD guided Tikhonov cross-validation for CCA.* We show that the truncated SVD CCA cross-validation can be computed more efficiently than the Tikhonov regularization path, at the price of a small loss in accuracy. In light of the spectral filtering interpretation we propose a hybrid algorithm that takes advantage of the fast computation of the regularization path of T-SVD CCA, in choosing a regularization parameter for the Tikhonov counterpart (Algorithm 4 in Appendix C), enabling a computationally lightweight exhaustive model selection, thanks to this hybrid strategy.

3) *Hierarchical Kernel Sentence Embedding and State of the art results.* We propose the Hierarchical Kernel Sentence Embedding (HKSE) as a means for aggregation of words embeddings (word2vec), that explains and outperforms the mean word2vec baseline. Using those features and mapping the search items to the query space via the asymmetric weighting of the Regularized CCA (T-SVD guided Tikhonov) and the cosine similarity, we achieve state of the art bidirectional retrieval results on the MSCOCO [12] and Flickr benchmarks [13, 14], with off the shelf features for image and text descriptions.

Notation. \mathcal{Q} and \mathcal{S} are query and search spaces. Given a multimodal training set $S = \{(x_i, y_i) | x_i \in \mathcal{X} \subset \mathbb{R}^{m_x}, y_i \in \mathcal{Y} \subset \mathbb{R}^{m_y}, i = 1 \dots n\}$, ($n > \max(m_x, m_y)$), let $X \in \mathbb{R}^{n \times m_x}$, and $Y \in \mathbb{R}^{n \times m_y}$ be the two data matrices corresponding to each modality. Define μ_X, μ_Y to be the means of X and Y respectively. Let $C_{XX} = X^T X - \mu_X \mu_X^T \in \mathbb{R}^{m_x \times m_x}$, and $C_{YY} = Y^T Y - \mu_Y \mu_Y^T \in \mathbb{R}^{m_y \times m_y}$ be the

covariances matrices of X and Y respectively. Let $C_{XY} = X^\top Y - \mu_X \mu_Y^\top \in \mathbb{R}^{m_x \times m_y}$ be the correlation matrix. Define I_k to be the identity matrix in k dimensions. SVD stands for the *thin* singular value decomposition. A validation set S_v is given for model selection. Our goal is to index a test set $S^* = \{(x_i^*, y_i^*) | x_i^* \in S_x^* \subset \mathcal{X}, y_i^* \in S_y^* \subset \mathcal{Y}, i = 1 \dots n^*\}$ for bidirectional search. X and Y are assumed to be centered. For X non singular, let $X = U\Sigma V^\top$, and $C_{XX} = X^\top X$, we define $C_{XX}^{-\frac{1}{2}} = V\Sigma^{-1}$. $\sigma_{x,1} \dots \sigma_{x,m_x}$ are singular values in decreasing order.

2. CCA and Image/Captions Bidirectional Retrieval

Bidirectional Retrieval. We start by defining more formally the bidirectional retrieval tasks. Given pairs of high dimensional points $(x_i, y_i) \in \mathcal{X} \times \mathcal{Y}$ where x_i corresponds to the feature representation of an image given by a deep convolutional neural network, and y_i a sentence embedding of an associated caption. Our goal is to index this multimodal data in a way that enables bidirectional retrieval: the image annotation task associating a caption to a query image and the image search task associating an image to a query caption.

Canonical Correlation Analysis. We review in this section Canonical Correlation Analysis due to [15]. For data matrices $X \in \mathbb{R}^{n \times m_x}$ and $Y \in \mathbb{R}^{n \times m_y}$, let $k = \min(m_x, m_y)$ the canonical correlations $\sigma_1, \dots, \sigma_k$, and their corresponding pairs of correlations weights $\{(u_i, v_i)\}_{i=1 \dots k}$, are given by the columns of $U \in \mathbb{R}^{m_x \times k}$ and $V \in \mathbb{R}^{m_y \times k}$, where U and V are the solution of the following maximization problem: $\max_{U^\top C_{XX} U = I_k, V^\top C_{YY} V = I_k} \text{Tr}(U^\top C_{XY} V)$, where $\sigma_i = u_i^\top C_{XY} v_i, i = 1 \dots k$. We note Σ the diagonal matrix having σ_i on its diagonal. Intuitively CCA finds the directions that are maximally correlated and that are orthonormal in the metric defined by each covariance matrix, respectively. Björk and Golub showed that the CCA problem is equivalent to the following formulation, minimizing the square of the Frobenius norm of the embeddings in the shared space:

$$\min_{U^\top C_{XX} U = I_k, V^\top C_{YY} V = I_k} \|XU - YV\|_F^2. \quad (1)$$

Cross-View Maps. Using the linear maps (U, V) from CCA, cross-view mapping of the multimodal data is defined as mapping the first modality to the second modality represented in the shared space. Interestingly we will see that those problems have a simple closed form solution using CCA. First for mapping images to captions embedded in the shared space we solve:

$$\min_{W_x \in \mathbb{R}^{m_x \times k}} \|XW_x - YV\|_F^2 \quad (2)$$

the minimum is achieved by (assuming X is non singular):

$$\begin{aligned} W_x &= (X^\top X)^{-1} X^\top YV = (X^\top X)^{-1} (X^\top X)U\Sigma \\ &= U\Sigma, \end{aligned}$$

where we used the property that CCA satisfies as a generalized eigenvalue problem [15] i.e $X^\top YV = (X^\top X)U\Sigma$. Second for mapping captions to the images embedded in the shared space we solve:

$$\min_{W_y \in \mathbb{R}^{m_y \times k}} \|YW_y - XU\|_F^2 \quad (3)$$

similarly the minimum is achieved by $W_y = V\Sigma$.

Those properties of cross-view mappings appeared for the first time in [16], for solving CCA in an alternating minimization fashion, we show in the following, that those properties are at the core of the bidirectional retrieval. Interestingly we see from solutions of Equations (2) and (3), that cross view maps between modalities and the shared space have a very simple form, suggesting embeddings having an asymmetric weighting of the canonical weights by the canonical correlations $(\Sigma U^\top, V^\top)$ and $(U^\top, \Sigma V^\top)$. We answer in this Section the following questions: *For a particular task which embedding should we use, the shared space embeddings (U^\top, V^\top) , or cross view mappings induced the by the asymmetric weighting? Given query and search spaces should the asymmetric weighting be on the query space or the search space canonical weight?*

We find empirically as discussed in Section 6 that asymmetric weighting should be on the search space, and not on the query space canonical weights. Moreover this particular asymmetric weighting outperforms unweighted CCA, as well as a symmetric weighting of CCA introduced in [7]. We give here an explanation of this empirical observation.

Shared Space Versus Cross-view Maps. To answer the first question, it is clear from the CCA formulation in Equation (1), that (U, V) are optimized jointly for both retrieval tasks, hence embeddings (U^\top, V^\top) are not optimized to their best for each task aside. On the other hand cross view maps in Equations (2) and (3) benefit from the shared space, and optimize for each task aside, hence are superior in bidirectional retrieval.

Query Generation Versus Search Generation. To answer the second question, this goes back to a fundamental problem in Information Retrieval. Given a query $q \in \mathcal{Q}$ and a search item $s \in \mathcal{S}$ (referred to usually as a document), two probabilistic retrieval approaches are possible [17]: 1) The Search Generation approach, modeling $\mathbb{P}(s|q)$ (*how likely is a search item given the query*) known as the traditional probabilistic approach 2) The query generation approach, modeling $\mathbb{P}(q|s)$ (*how likely is a query item given a search item*), known also as the language modeling approach. Lafferty

et al [17] showed that while both approaches are equivalent probabilistically as they are based on a different parametrization of a same joint *relevance* likelihood, they are different statistically as the models are estimated differently. [17] propose to use a binary random variable r that denotes relevance between a query and a search item, $r = 1$ if there is a match and 0 otherwise. In order to rank search items [17] propose the use of the log-odds ratio: $\log \frac{\mathbb{P}(r=1|q,s)}{\mathbb{P}(r=0|q,s)}$. Using the search generation approach this ratio is equivalent to [17]: $\log \frac{\mathbb{P}(s|q,r=1)}{\mathbb{P}(s|q,r=0)}$, hence this approach needs both positives and negatives pairs of search and query items (triplet losses are instances of this approach). On the other hand using the query generation approach (under mild assumptions) this ratio is equivalent to [17]: $\log \mathbb{P}(q|s, r = 1)$.

As shown in [17] the query generation approach models relevance in an implicit way and does not need negative samples. The implicit relevance modeling makes the query generation approach appealing and we adopt it in the rest of this paper. Consider for instance the image search task (text query, image search space) considering a gaussian model in the query generation approach: $q = V^\top y \sim \mathcal{N}(W_x^\top x, \sigma^2 I_k)$, $\sigma > 0$, $s = x$. Maximizing the log likelihood of this query generation approach corresponds to Equation (2) and the optimal W_x is given by $U\Sigma$. Hence for the image search task we can use the embeddings $(\Sigma U^\top, V^\top)$, and the image search problem reduces to finding for a query caption $y^* \in S_y^*$, an image $x^* \in S_x^*$ using ℓ_2 or cosine similarity, i.e $\arg \min_{x^* \in S_x^*} \|\Sigma U^\top x^* - V^\top y^*\|_2^2$ or,

$$\arg \max_{x^* \in S_x^*} \frac{\langle \Sigma U^\top x^*, V^\top y^* \rangle}{\|\Sigma U^\top x^*\|_2 \|V^\top y^*\|_2}. \quad (4)$$

Similarly for the image annotation problem we can use the embeddings $(U^\top, \Sigma V^\top)$, and it reduces also to finding for a query image $x^* \in S_x^*$, and a caption $y^* \in S_y^*$ using ℓ_2 or cosine similarity, i.e $\arg \min_{y^* \in S_y^*} \|U^\top x^* - \Sigma V^\top y^*\|_2^2$ or,

$$\arg \max_{y^* \in S_y^*} \frac{\langle U^\top x^*, \Sigma V^\top y^* \rangle}{\|U^\top x^*\|_2 \|\Sigma V^\top y^*\|_2}. \quad (5)$$

Thus using the query generation approach we see that Σ appears in an asymmetric way in the embedding of the points depending on the task: the canonical weight of the search space is weighted by the canonical correlations. Hence we call our method asymmetrically weighted CCA (Table 1)

| Task | Image Embedding | Caption Embedding |
|------------|---------------------|---------------------|
| Search | $\Sigma U^\top x^*$ | $V^\top y^*$ |
| Annotation | $U^\top x^*$ | $\Sigma V^\top y^*$ |

Table 1: Asymmetrically Weighted CCA: Task dependent embeddings, in the query generation approach. x^* is a test image, y^* is a test caption. (U, V) are the canonical weights of X and Y . Σ is the diagonal canonical correlations matrix.

Remark 1 1) We found in practice that the cosine similarity between the embeddings outperforms ℓ_2 based retrieval. This is in line with findings in the CCA based retrieval where cosine similarities are used [5], [7] and reported to be outperforming ℓ_2 . 2) Intuitively, in the query generation approach, the canonical correlations weigh the search canonical weights directions. This weighting will favor search canonical directions that are highly correlated with the query. Hence every search item is strengthened and asked to match the query. In the search generation approach, the canonical correlations weigh the query canonical weights directions. The query will get strengthened alone and asked to match all search items, which hints to why this approach is weaker : distributing strength on all search items (query generation approach), is better than stressing it on the query alone (Search generation approach).

3. CCA Computation and Regularization

In this section we focus on the computational aspects of CCA and its regularization. CCA can be solved as a generalized eigenvalue problem or using singular value decomposition by virtue of the Björk Golub algorithm. As we will see in this Section solving using SVD offers computational advantages, and allows for regularization using spectral filtering techniques.

Björk Golub Algorithm. The following Lemma due to Björk and Golub shows that the canonical correlation weights can be computed using SVD:

Lemma 1 ([10]) Let $X = U_x \Sigma_x V_x^\top$, and $Y = U_y \Sigma_y V_y^\top$ be the singular value decomposition of X and Y ($U_x \in \mathbb{R}^{n \times m_x}$, $\Sigma_x \in \mathbb{R}^{m_x \times m_x}$, $V_x \in \mathbb{R}^{m_x \times m_x}$). Let $k = \min(m_x, m_y)$, and $T = U_x^\top U_y$. Let $T = P_x \Sigma P_y^\top$ be its SVD, $P_x \in \mathbb{R}^{m_x \times k}$, $\Sigma \in \mathbb{R}^{k \times k}$, $P_y \in \mathbb{R}^{m_y \times k}$. The canonical correlations of X and Y are the diagonal elements of Σ , with canonical weights of X given by $U = V_x \Sigma_x^{-1} P_x$, and the canonical weights of Y given by $V = V_y \Sigma_y^{-1} P_y$. (Proof in Appendix B).

Algorithm 1 (Appendix C) summarizes the Björk Golub procedure to compute CCA. The total computational complexity of this algorithm assuming $m_y < m_x$ is $O(nm_x^2 + nm_y^2 + m_x m_y^2)$. For now we have assumed that the covariances C_{XX} and C_{YY} are non-singular, and we presented an SVD version of the Björk Golub Algorithm in this context. Regularizing CCA does not only allow for numerical stability in the non singular case, it also allows for better generalization properties and avoids overfitting.

Tikhonov and Truncated SVD Regularization. The Tikhonov regularized CCA problem [9] for parameters $\gamma_x, \gamma_y > 0$ can be written in this form:

$$U^\top (X^\top X + \gamma_x I_{m_x}) U = I_k, V^\top (Y^\top Y + \gamma_y I_{m_y}) V = I_k \quad \max_{U, V} \text{Tr}(U^\top X^\top Y V). \quad (6)$$

Let $k_x \leq m_x$ and let X_{k_x} be the best k_x -rank approximation of X given by the truncated SVD: $X_{k_x} = U_{k_x} \Sigma_{k_x} V_{k_x}^\top$, $U_{k_x} \in \mathbb{R}^{n \times k_x}$, $\Sigma_{k_x} \in \mathbb{R}^{k_x \times k_x}$, $V_{k_x} \in \mathbb{R}^{m_x \times k_x}$. Similarly for Y , we define the best k_y -rank approximation ($k_y \leq m_y$): $Y_{k_y} = U_{k_y} \Sigma_{k_y} V_{k_y}^\top$, $U_{k_y} \in \mathbb{R}^{n \times k_y}$, $\Sigma_{k_y} \in \mathbb{R}^{k_y \times k_y}$, $V_{k_y} \in \mathbb{R}^{m_y \times k_y}$. We define the truncated SVD CCA as follows:

$$U^\top X_{k_x}^\top X_{k_x} U = I_{k_x}, V^\top Y_{k_y}^\top Y_{k_y} V = I_{k_y} \quad (7)$$

The following Theorem Proved in Appendix B shows how the Björk-Golub procedure to compute the canonical weights extends to the regularized case, using singular value decompositions of the data matrices and a correlation operator.

Theorem 1 (Regularized CCA) Let $X = U_x \Sigma_x V_x^\top$, and $Y = U_y \Sigma_y V_y^\top$ be the singular value decomposition of X and Y ($U_x \in \mathbb{R}^{n \times m_x}$, $\Sigma_x \in \mathbb{R}^{m_x \times m_x}$, $V_x \in \mathbb{R}^{m_x \times m_x}$).

1. *Tikhonov Regularization.* Let $k = \min(m_x, m_y)$. Define the Tikhonov regularized correlation operator

$$T_{\gamma_x, \gamma_y} = (\Sigma_x^2 + \gamma_x I)^{-\frac{1}{2}} \Sigma_x (U_x^\top U_y) \Sigma_y (\Sigma_y^2 + \gamma_y I)^{-\frac{1}{2}},$$

and let $T_{\gamma_x, \gamma_y} = P_x \Sigma P_y^\top$ be its singular value decomposition ($P_x \in \mathbb{R}^{m_x \times k}$, $\Sigma \in \mathbb{R}^{k \times k}$, $P_y \in \mathbb{R}^{m_y \times k}$). The canonical weights of the Tikhonov regularized CCA (6) are given by $U = V_x (\Sigma_x^2 + \gamma_x I)^{-\frac{1}{2}} P_x$ and $V = V_y (\Sigma_y^2 + \gamma_y I)^{-\frac{1}{2}} P_y$. Canonical correlations are given by Σ .

2. *Truncated SVD Regularization.* Define the T-SVD regularized correlation operator $T_{k_x, k_y} = U_{k_x}^\top U_{k_y}$, and let $T_{k_x, k_y} = P_x \Sigma P_y^\top$ be its singular value decomposition. The canonical weights of the T-SVD regularized CCA (7) are given by $U = V_{k_x} \Sigma_{k_x}^{-1} P_x$ and $V = V_{k_y} \Sigma_{k_y}^{-1} P_y$. Canonical correlations are given by Σ .

3. *Spectral Filtering.* (Tikhonov) Define f_{γ_x} a spectral filter acting on the singular values of X , such that $f_{\gamma_x, j} = \frac{\sigma_{x,j}}{\sqrt{\sigma_{x,j}^2 + \gamma_x}}$, $j = 1 \dots m_x$. Similarly define f_{γ_y} . we have:
$$T_{\gamma_x, \gamma_y} = f_{\gamma_x}(\Sigma_x) U_x^\top U_y f_{\gamma_y}(\Sigma_y). \quad (8)$$

(T-SVD) Define f_{k_x} an element wise filter acting on the singular values of X , such that: $f_{k_x}(\sigma_{x,j}) = 0$ if $\sigma_{x,j} < \sigma_{x, k_x}$, and $f_{k_x}(\sigma_{x,j}) = 1$ if $\sigma_{x,j} \geq \sigma_{x, k_x}$. Let $T_f^{k_x, k_y} = f_{k_x}(\Sigma_x) U_x^\top U_y f_{k_y}(\Sigma_y)$, For a matrix A , $A(1 : k_x, 1 : k_y)$, refers to the sub-matrix containing the first k_x rows and the first k_y columns of A . We have:

$$T_{k_x, k_y} = T_f^{k_x, k_y}(1 : k_x, 1 : k_y). \quad (9)$$

Spectral Filtering for CCA. From Equations (8) and (9) we see that both regularizations are proceeding by filtering of singular values. While T-SVD proceeds by a hard filtering, Tikhonov proceeds with a soft filtering. In order to see the correspondence between T-SVD and Tikhonov regularization it is important to consider the following choice of regularization parameters: For a choice of (k_x, k_y) in T-SVD, consider $\gamma_x = \sigma_{x, k_x}^2$ and $\gamma_y = \sigma_{y, k_y}^2$ in Tikhonov Regularization. With this particular choice the spectral filters for Tikhonov regularization become: $f_{\sigma_{k_x}^2}(\sigma_{x,j}) = \frac{\sigma_{x,j}}{\sqrt{\sigma_{x,j}^2 + \sigma_{x, k_x}^2}}$. Let $\alpha > 0$, consider: 1) $g_{\text{hard}}(x) = 0$, if $0 \leq x < \alpha$, and $g_{\text{hard}}(x) = 1$ if $x \geq \alpha$. 2) $g_{\text{soft}}(x) = \frac{x}{\sqrt{x^2 + \alpha^2}}$. It is easy to see that Equations (8) and (9), correspond to the element-wise application of g_{hard} and g_{soft} respectively for $\alpha = \sigma_{k_x}$ (See Figure 1 for g_{hard} versus g_{soft} , for $\alpha = 20$). In conclusion, using this

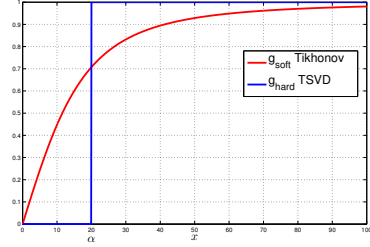


Figure 1: Both T-SVD and Tikhonov Regularization correspond to a spectral filtering of the singular values of X and Y . T-SVD is a hard pruning of directions corresponding to singular values less than the threshold defined by σ_{k_x} . For $\alpha = \sigma_{k_x}$ Tikhonov corresponds to a soft pruning of those directions.

spectral filtering approach the natural set of regularization parameters for Tikhonov regularization (γ_x, γ_y) is therefore the set of singular values squared of X and Y respectively. Hence in order to cross-validate CCA we propose the following three approaches:

- 1) **Tikhonov-CCA:** Perform a grid search on $(\gamma_x, \gamma_y) \in \{\sigma_{1,x}^2, \dots, \sigma_{m_x,x}^2\} \times \{\sigma_{1,y}^2, \dots, \sigma_{m_y,y}^2\}$, using the SVD of T_{γ_x, γ_y} . Each SVD costs $\min(O(m_x m_y^2), O(m_y m_x^2))$ (Algorithm 2 in Appendix C).
- 2) **T-SVD-CCA:** Perform a grid search on $(k_x, k_y) \in [1, m_x] \times [1, m_y]$, using the SVD of T_{k_x, k_y} . This grid search (Algorithm 3 in Appendix C) is computationally efficient since each SVD costs $\min(O(k_x k_y^2), O(k_y k_x^2))$, hence more efficient than Tikhonov.
- 3) **G-Tikhonov-CCA:** While there is no exact one to one correspondence between the soft pruning and the hard pruning in T-SVD and Tikhonov, the spectral filtering interpretation suggests that the optimal (k_x^*, k_y^*) from T-SVD cross-validation (computationally efficient), can be used as a proxy for the optimal Tikhonov cross validation (computationally expensive), by simply setting $(\gamma_x, \gamma_y) = (\sigma_{x, k_x^*}^2, \sigma_{y, k_y^*}^2)$ with

a small loss in the accuracy. This is summarized in Algorithm 4 in Appendix C. Algorithm 4, takes advantage of the fast computation of T-SVD regularization for CCA, and the spectral filtering interpretation in order to choose a good regularization parameter for Tikhonov Regularization.

4. Hierarchical Kernel Sentence Embedding

Features. After proposing our asymmetric CCA and an efficient way to cross validate it for bidirectional retrieval of images and sentences, we address in this Section the question of feature representation for both modalities. Convolutional neural networks are the gold standard in computer vision, hence we focus here on defining a new sentence embedding for aggregating local features in text description. Given a vocabulary \mathcal{A} represented by a vector space i.e a word embedding, word2vec for instance [18], a sentence can be seen as a distribution ρ on \mathcal{A} .

A Kernel between Distributions. Given a distribution ρ defined on a vocabulary space $\mathcal{A} \subset \mathbb{R}^d$. Let $k_{\gamma,d}$ be a shift invariant kernel such as the gaussian kernel with parameter γ , for $a, b \in \mathcal{A}$, $k_{\gamma,d}(a, b) = \exp(-\frac{\gamma}{2} \|a - b\|^2)$. Let \mathcal{H}_k be the associated Reproducing Kernel Hilbert Space (RKHS), with norm $\|\cdot\|_{\mathcal{H}_k}$. The kernel mean embedding of ρ is defined [19] as follows $\mu(\rho) = \int_{\mathcal{A}} k_{\gamma,d}(a, \cdot) \rho(a) da$. $\mu \in \mathcal{H}_k$ and can be used to define a distance between two distributions ρ_1 and ρ_2 by means of $\|\mu(\rho_1) - \mu(\rho_2)\|_{\mathcal{H}_k}^2$. Given a finite sample $\{a_1, \dots, a_n\}$ from ρ the empirical kernel mean embedding is given by: $\mu_n(\rho) = \frac{1}{n} \sum_{i=1}^n k_{\gamma,d}(a_i, \cdot)$. Let $\eta > 0$, define the following kernel [19, 20, 21] between distributions ρ_1 and ρ_2 defined on \mathcal{A} , given a finite sample $\{a_1 \dots a_{n_1}\}$ and $\{b_1 \dots b_{n_2}\}$ from each distribution respectively:

$$K(\rho_1, \rho_2) = \exp\left(-\frac{\eta}{2} \|\mu_{n_1}(\rho_1) - \mu_{n_2}(\rho_2)\|_{\mathcal{H}_k}^2\right).$$

It is easy to see that $K(\rho_1, \rho_2) = \exp\left(\frac{\eta}{2} \Delta\right)$, where $\Delta = \frac{1}{n_1 n_2} \sum_{i=1}^{n_1} \sum_{j=1}^{n_2} 2k_{\gamma,d}(a_i, b_j) - \frac{1}{n_1^2} \sum_{i,j=1}^{n_1} k_{\gamma,d}(a_i, a_j) - \frac{1}{n_2^2} \sum_{i,j=1}^{n_2} k_{\gamma,d}(b_i, b_j)$. A sentence with words $a_i, i = 1 \dots n$ embedded in \mathcal{A} , can be seen as a set of finite samples from a distribution ρ . Hence to compare two sentences we can use the kernel K defined above. Note that K is the composition of a word level similarity where a pairwise comparison (intra and inter sentences) of words is computed using a first level gaussian kernel, and a sentence level similarity on the average pairwise similarity of words using a second level gaussian kernel.

Hierarchical Kernel Sentence Embedding (HKSE).

Rather than using the kernel K and kernel CCA, that are computationally expensive, we make use of random Fourier features [22] in approximating K with an explicit feature map i.e a sentence embedding. Let $\Phi_{\gamma,d}(a) \in \mathbb{R}^m$, $\Phi_{\gamma,d}(a) = \frac{\sqrt{2}}{\sqrt{m}} (\cos(\langle w_1, a \rangle + b_1) \dots \cos(\langle w_m, a \rangle +$

$b_m))$, $w_j \sim \mathcal{N}(0, \gamma I_d)$, and $b \sim \text{Unif}[0, 2\pi]$, we have $\langle \Phi_{\gamma,d}(a), \Phi_{\gamma,d}(b) \rangle \approx k_{\gamma,d}(a, b)$. Hence we define the randomized kernel mean map of ρ , $\hat{\mu}_n(\rho) = \frac{1}{n} \sum_{i=1}^n \Phi_{\gamma,d}(a_i)$. For sufficiently large m we have

$$K(\rho_1, \rho_2) \approx k_{\eta,m}(\hat{\mu}_{n_1}(\rho_1), \hat{\mu}_{n_2}(\rho_2)).$$

$k_{\eta,m}$ is also a shift invariant kernel in m dimension, that can be in its turn approximated with a random feature map $\Phi_{\eta,m} \in \mathbb{R}^{m'}$. For sufficiently large m' , we have

$$K(\rho_1, \rho_2) \approx \langle \Phi_{\eta,m}(\hat{\mu}_{n_1}(\rho_1)), \Phi_{\eta,m}(\hat{\mu}_{n_2}(\rho_2)) \rangle_{\mathbb{R}^{m'}}.$$

Hence K is approximated by a deep (2 layers) map, that is the composition of a non linear average pooling and a non linear feature map. By embedding sentences consisting of word vectors (word2vec) $a_1 \dots a_n$ using $\Phi_{\eta,m}(\frac{1}{n} \sum_{i=1}^n \Phi_{\gamma,d}(a_i))$, we compute implicitly the similarity K between the bag of words distributions. While $k_{\gamma,d}$ or $\Phi_{\gamma,d}$ act as a localizer at the word level, $k_{\eta,m}$ or $\Phi_{\eta,m}$ localize on the sentence level. Hence we note them respectively with k^w, Φ^w (word level kernel), and k^s, Φ^s (sentence level kernel). We note the embedding with $\text{HKSE}(k^w, k^s)$. The average word2vec representation proposed in [5] corresponds to $\text{HKSE}(k^w, k^s)$, where k^w and k^s are linear kernels. The following proposition proved in Appendix E.1 gives bounds on m and m' :

Proposition 1 (HKSE approximation) *Let \mathcal{A} be the vocabulary embedded in a vector space. Let $|\mathcal{A}|$ be the size of the vocabulary. Let s be the maximum sentence length. Let $\hat{\mu}_{n_1}(\rho_1) = \frac{1}{n_1} \sum_{i=1}^{n_1} \Phi_{\gamma,d}(a_i)$, and $\hat{\mu}_{n_2}(\rho_2) = \frac{1}{n_2} \sum_{i=1}^{n_2} \Phi_{\gamma,d}(b_i)$, on two different sentences ρ_1, ρ_2 , with words $\{a_1, \dots, a_{n_1}\}$ and $\{b_1, \dots, b_{n_2}\}$ respectively. Let $\hat{K}(\rho_1, \rho_2) = \langle \Phi_{\eta,m}(\hat{\mu}_{n_1}(\rho_1)), \Phi_{\eta,m}(\hat{\mu}_{n_2}(\rho_2)) \rangle$. Let $\epsilon, \delta > 0$, for $m \geq \frac{1}{2\delta^2} \log(|\mathcal{A}|^2/\epsilon)$ and $m' \geq \frac{1}{2\delta^2} \log(|\mathcal{A}|^{2s}/\epsilon)$ we have with probability $1 - 2\epsilon$: $\frac{1}{c(\eta,\delta)} K(\rho_1, \rho_2) - \delta \leq \hat{K}(\rho_1, \rho_2) \leq c(\eta, \delta) K(\rho_1, \rho_2) + \delta$, where $c = \exp(\frac{3\eta\delta}{2})$.*

Informally for the 2 layers kernel the estimation error is multiplicative and additive. The inner word level dimension of HKSE scales logarithmically with the vocabulary size $m = O(\log(|\mathcal{A}|))$, and the outer dimension scales linearly with the maximum sentence length s as logarithmically with the vocabulary size $m' = O(s \log(|\mathcal{A}|))$.

Remark 2 *We give in Appendix E.2 a probabilistic interpretation of HKSE as a Gaussian Embedding of sentences.*

5. Relation to Previous work

We focus in this section on some recent works that use bidirectional maps in the retrieval tasks and their relation to this paper. [5], and [7] used CCA to build a joint representation using the cosine similarity. In both works a symmetric

weighting of the CCA canonical weights was used, i.e for an image caption pair (x^*, y^*) , a joint embedding of the form $(\Sigma^\alpha U^\top x^*, \Sigma^\alpha V^\top y^*)$, was used, where $\alpha = 0$, in the case of [5] and $\alpha > 0$ in the case of [7]. The symmetric weighting in [7] was found to improve performance and is not theoretically motivated as in the asymmetric weighting of this paper. Indeed our experimental results show that asymmetric weighting gives higher performance. Skip thought vectors introduced in [6] for representing sentences were used for bidirectional search in conjunction with VGG features [23] on the image side, with linear embeddings learned with a discriminative triplets loss, instead of a CCA loss. Order embeddings introduced in [24] uses an order similarity rather than the cosine similarity and learns an end to end sentence embedding with an LSTM. Another end to end approach using deep neural networks on image and text features under a structured loss was introduced [25].

6. Numerical Results

Datasets. We performed image annotation and search tasks on the MSCOCO benchmark [12], and Flickr 8K and 30 K benchmarks [13, 14] using our task dependent asymmetrically weighted CCA, as described in Table 1. Retrieval was performed using cosine similarities given in Equations (4) and (5). For details on data splits and experimental protocol check Appendix F. We report for both tasks the recall rate at one result, five results, or ten first results ($r@1,5,10$), as well as the median rank of the first ground truth retrieval on the test set.

Image/Text Features. For feature extraction we follow [5], and use on the image side the VGG CNN representation [23], where each image was rescaled to have smallest side 384 pixels, and then cropped in 10 ways into 224 by 224 pixel images: the four corners, the center, and their x-axis mirror image. The mean intensity of each crop is subtracted in each color channel, and then encoded by VGG19 (the final FC-4096 layer). The average of the resulting 10 feature vectors corresponding to each crop is used as the image representation. We also use the residual convolutional neural network Resnet101 (101 layers)[26]. We don't rescale or crop the image, we encode the full size image with the Resnet and apply spatial average pooling to the last layer resulting in a vector of dimension $m_x = 2048$. On the text side, we use two sentence embeddings 1) HKSE(k^w, k^s), introduced in this paper, using word2vec available on code.google.com/p/word2vec/ (throughout our experiments, γ was set to be the inverse of the squared median pairwise distances of words in the vocabulary, η was fixed to 0.01, for MSCOCO we use $m = 2000$ and $m' = 3000$, for Flickr we use $m = 2000$ and $m' = 2000$). Note that HKSE(lin,lin), corresponds to the mean word2vec baseline as in [5]. 2) Skip thought vectors introduced in [6], which encodes sentences

to vectors using an LSTM. Image and text features were centered before learning CCA. For AW-CCA we used cosine similarity that we find to outperform ℓ_2 , and performed search and annotation as given in Equations (4), and (5) respectively.

Empirical Validation of Our Approach.

We confirm in this section empirically our main claims and contributions:

1) *Query Generation Versus Search Generation:* In order to confirm our claims in Section 2, on the optimality of the asymmetric weighting in the query generation approach, we perform bidirectional retrieval on MS-COCO using image embedding of the form $\Sigma^\alpha U^\top$ and caption embedding of the form $\Sigma^{1-\alpha} V^\top$, where $\alpha \in [0, 1]$. We plot in Figure 2 $r@10$ versus α on the validation set, for image annotation and image search. The cosine similarity was used between embeddings. In this experiment we used VGG image features and average word2vec sentence embedding. For each α we perform a thorough cross validation using truncated SVD CCA, and report the best $r@10$ for image annotation and image search. We see that $\alpha = 0$, i.e the embedding $(U^\top, \Sigma V^\top)$ is optimal for image annotation as predicted by the query generation approach for image annotation. Similarly we see that $\alpha = 1$, i.e the embedding $(\Sigma U^\top, V^\top)$, is optimal for image search. This confirms our claim that the asymmetric weighting should be on the search space. To illustrate the organization of the space with asymmetric CCA, we refer the reader to t-SNE plots in Appendix D.

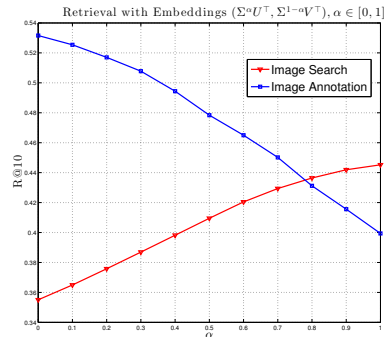


Figure 2: Optimality of the asymmetric weighting in the query generation approach.

2) *Asymmetric Weighting versus CCA and Symmetric Weighting:* On MS-COCO, using same VGG/average word2vec features, we perform bidirectional retrieval using embeddings of the form $(\Sigma^\alpha U^\top, \Sigma^\alpha V^\top)$. Note that $\alpha = 0$ corresponds to CCA as used in [5], and $\alpha > 0$ corresponds to the symmetric weighting introduced in [7], we see in Table 2 that AW-CCA outperforms both approaches.

3) *Guided Tikhonov Cross Validation Speed/Performance*

| | Image search | | | Image annotation | | |
|---|--------------|-------|-------|------------------|-------|-------|
| | r@1 | r@5 | r@10 | r@1 | r@5 | r@10 |
| Symmetric Weighting | | | | | | |
| $(\Sigma^\alpha U^\top, \Sigma^\alpha V^\top), \alpha = 0$ (CCA) | 9.36 | 26.13 | 37.30 | 13.96 | 34.30 | 47.10 |
| $(\Sigma^\alpha U^\top, \Sigma^\alpha V^\top), \alpha = 1$ | 11.21 | 28.95 | 40.24 | 13.72 | 34.00 | 45.86 |
| $(\Sigma^\alpha U^\top, \Sigma^\alpha V^\top), \alpha = 2$ | 10.04 | 26.54 | 37.46 | 11.16 | 29.02 | 39.56 |
| $(\Sigma^\alpha U^\top, \Sigma^\alpha V^\top), \alpha = 3$ | 8.30 | 23.53 | 33.78 | 9.36 | 24.74 | 35.56 |
| $(\Sigma^\alpha U^\top, \Sigma^\alpha V^\top), \alpha = 4$ | 7.09 | 20.79 | 30.81 | 7.88 | 21.58 | 32.22 |
| $(\Sigma^\alpha U^\top, \Sigma^\alpha V^\top), \alpha = 5$ | 6.16 | 18.63 | 27.79 | 6.76 | 19.76 | 29.46 |
| $(\Sigma^\alpha U^\top, \Sigma^\alpha V^\top), \alpha = 6$ | 5.55 | 16.76 | 25.31 | 6.08 | 17.80 | 27.12 |
| Task Dependent Asymmetric Weighting: | | | | | | |
| Image Search: $(\Sigma U^\top, V^\top)$, Image Annotation: $(U^\top, \Sigma V^\top)$ | 12.92 | 32.38 | 44.52 | 17.84 | 40.42 | 53.16 |

Table 2: The asymmetric weighting we propose outperforms the symmetric weighting [7] and CCA as shown in this table, and boosts performance (retrieval rates in %) of both tasks.

Tradeoff: We report in Table 3 the timing (in hours) of computing regularization path of AW-CCA, with T-SVD and Tikhonov, on MSCOCO. The parameter grid for both cases is 20×20 . Experiments were conducted on a single Intel Xeon CPU E5-2667, 3.30GHz, with 265 GB of RAM and 25.6 MB of cache. We see that T-SVD is faster to cross validate than Tikhonov : 2x speedup for VGG/w2v ($m_x=4096, m_y=300$), 6x speedup for VGG/skip thoughts ($m_x=4096, m_y=4800$). Thanks to the speed advantage of T-SVD we confirm that T-SVD Guided Tikhonov regularization introduced in Section 3 incurs a small loss in accuracy with respect to full Tikhonov validation on Flickr 30K dataset.

| AW- CCA | CPU time |
|-------------------------|----------|
| T-SVD (VGG/w2v) | 1.04 h |
| Tikhonov- CCA (VGG/w2v) | 1.94 h |
| T-SVD (VGG/Skip) | 6.92 h |
| Tikhonov (VGG/Skip) | 45.31 h |

Table 3: Timing in hours of CCA Cross Validation: T-SVD versus Tikhonov.

| AW-CCA | Image search | | | Image annotation | | |
|--------|--------------|--------------|--------------|------------------|--------------|--------------|
| | r@1 | r@5 | r@10 | r@1 | r@5 | r@10 |
| Tikh | 23.08 | 50.62 | 63.53 | 30.66 | 59.1 | 70.13 |
| T-SVD | 20.61 | 46.91 | 59.9 | 27.0 | 55.5 | 67.80 |
| G-Tikh | 22.40 | 49.94 | 62.62 | 30.56 | 58.43 | 69.96 |

Table 4: Mean results (in %) of the test splits on the Flickr 30 K, in average VGG/ Average w2vec setup. We see that G-Tikh and Tikh are on par.

Discussion of the Results. We report here our results using the Asymmetrically Weighted TSVD-Guided-Tikhonov CCA (AW-G-Tikh-CCA) given in Algorithm 4 (Appendix

C) where we select the model corresponding to the maximum r@1 on the validation set (regularization paths are given in Appendix G). When we use VGG for image encoding we observe in Tables 5 and 6 that 1) AW-G-Tikh-CCA with the same Mean Vec features (HKSE(lin,lin)) outperforms consistently the CCA baseline in [5], this is mainly due to the asymmetric weighting and the query generation approach, as well as the efficient model selection introduced in this paper. 2) HKSE(rbf,rbf) consistently outperforms the mean vector baseline as well as skip thoughts vectors and can be used therefore as a simple yet strong off the shelf sentence embedding. HKSE(rbf,rbf) outperforms the fisher vector representation [5], on the MSCOCO Benchmark. Note that, Fisher vectors are learned on the dataset, and HKSE is fully unsupervised. For the same image features (VGG) end to end order embeddings (VGG)[24] outperforms HKSE on image search on COCO. We see from Tables 5 and 6 that encoding images with Resnet and spatial average pooling, in conjunction with the concatenation of [HSKE(lin,rbf)||HKSE(rbf,rbf)] boosts the performance of AW-CCA and achieve state of the art performance on both tasks. Note that we get significant boosts on both image search and annotation tasks since the asymmetric weighting of CCA gives us for free an optimized system for each task, while competing methods optimize jointly for both tasks using the same embeddings.

7. Conclusion

In this paper we showed that the query generation approach in information retrieval [17], can be applied to bidirectional retrieval, where we map the search space to the query space via an asymmetric weighting of regularized CCA. Asymmetric weighting improves the performance of the bidirectional retrieval tasks. We also presented a computationally efficient cross validation for regularized CCA, that

| | Image search | | | | Image annotation | | | |
|---|--------------|--------------|--------------|------------|------------------|--------------|--------------|------------|
| | r@1 | r@5 | r@10 | med r | r@1 | r@5 | r@10 | med r |
| 1K test images: | | | | | | | | |
| CCA+ Mean Vec [5] | 24.2 | 56.4 | 72.4 | 4.0 | 33.2 | 61.8 | 75.1 | 3.0 |
| AW-G-Tikh-CCA +VGG+ HKSE(lin,lin) (Mean Vec) | 28.14 | 61.33 | 76.64 | 3.0 | 37.16 | 68.78 | 81.36 | 2.0 |
| AW-G-Tikh-CCA+VGG+HKSE (lin,rbf) | 30.99 | 65.43 | 79.49 | 3.0 | 39.94 | 71.82 | 84.1 | 2.0 |
| AW-G-Tikh-CCA+VGG+HKSE (rbf,lin) | 29.54 | 63.79 | 78.70 | 3.0 | 41.10 | 70.90 | 82.46 | 2.0 |
| AW-G-Tikh-CCA+VGG+HKSE (rbf,rbf) | 32.70 | 67.51 | 81.14 | 3.0 | 43.64 | 74.94 | 85.68 | 2.0 |
| AW-G-Tikh-CCA+VGG+[HKSE (lin,rbf)∥HKSE(rbf,rbf)] | 34.84 | 69.92 | 82.73 | 3.0 | 46.54 | 77.50 | 87.22 | 2.0 |
| AW-G-Tikh-CCA+ResNet+HKSE (lin,lin) | 32.95 | 67.12 | 81.07 | 3.0 | 43.1 | 75.92 | 87.24 | 2.0 |
| AW-G-Tikh-CCA+ResNet+[HKSE (lin,rbf)∥HKSE(rbf,rbf)] | 39.68 | 73.98 | 86.23 | 2.0 | 55.16 | 83.84 | 92.52 | 1.0 |
| AW-G-Tikhonov-CCA+VGG+Skip thoughts | 29.14 | 63.74 | 77.53 | 3.0 | 39.24 | 70.44 | 82.68 | 2.0 |
| Triplets loss +VGG+Skip thoughts [6] | 25.9 | 60 | 74.6 | NA | 33.8 | 67.7 | 82.1 | NA |
| BRNN+VGG [1] | 20.9 | 52.8 | 69.2 | 4.0 | 29.4 | 62.0 | 75.9 | 2.5 |
| CCA +VGG+Fisher GMM+HGLMM [5] | 25.6 | 60.4 | 76.8 | 4.0 | 38.9 | 68.4 | 80.1 | 2.0 |
| Order Embedding+VGG [24] | 37.9 | NA | 85.9 | 2.0 | 46.7 | NA | 88.9 | 2.0 |
| 5K test images: | | | | | | | | |
| CCA +VGG+Mean Vec [5] | 10.3 | 27.2 | 38.4 | 18.0 | 12.8 | 32.1 | 44.6 | 14.0 |
| AW-G-Tikh-CCA +VGG+HKSE(lin,lin) (Mean Vec) | 12.91 | 32.17 | 44.24 | 14.0 | 17.9 | 40.30 | 53.12 | 9.0 |
| AW-G-Tikh-CCA+VGG +HKSE (lin,rbf) | 14.24 | 35.39 | 48.34 | 11.0 | 19.06 | 43.02 | 57.02 | 8.0 |
| AW-G-Tikh-CCA+VGG+HKSE (rbf,lin) | 13.46 | 33.74 | 46.08 | 13.0 | 19.98 | 44.50 | 56.90 | 7.0 |
| AW-G-Tikh-CCA+VGG+HKSE (rbf,rbf) | 15.44 | 37.44 | 50.69 | 10.0 | 22.14 | 47.76 | 60.68 | 6.0 |
| AW-G-Tikh-CCA+VGG+[HKSE (lin,rbf)∥HKSE(rbf,rbf)] | 16.63 | 40.35 | 53.60 | 9.0 | 23.70 | 50.32 | 63.14 | 5.0 |
| AW-G-Tikh-CCA+ResNet+HKSE (lin,lin) | 15.69 | 37.64 | 50.29 | 10.0 | 22.58 | 47.3 | 60.98 | 6.0 |
| AW-G-Tikh-CCA+ResNet+[HKSE (lin,rbf)∥HKSE(rbf,rbf)] | 20.22 | 45.05 | 58.53 | 7.0 | 31.48 | 60.54 | 72.32 | 3.0 |
| AW-G-Tikhonov-CCA+VGG+Skip thoughts | 12.83 | 33.73 | 47.04 | 12.0 | 18.5 | 42.24 | 55.34 | 8.0 |
| Triplets loss +VGG+Skip thoughts [6] | NA | NA | NA | NA | NA | NA | NA | NA |
| BRNN+VGG [1] | 8.9 | 24.9 | 36.3 | 19.5 | 11.8 | 32.5 | 45.4 | 12.2 |
| CCA +VGG+Fisher GMM+HGLMM [5] | 11.2 | 29.2 | 41.0 | 16.0 | 17.7 | 40.1 | 51.9 | 10.0 |
| Order Embedding+VGG [24] | 18.0 | NA | 57.6 | 7.0 | 23.3 | NA | 65 | 5.0 |

Table 5: Mean results of the test splits on the MSCOCO benchmark (in %).

| | Image search | | | | Image annotation | | | |
|---|--------------|--------------|--------------|------------|------------------|--------------|--------------|------------|
| | r@1 | r@5 | r@10 | med r | r@1 | r@5 | r@10 | med r |
| Flickr 30 K | | | | | | | | |
| CCA + VGG+Mean Vec [5] | 20.5 | 46.3 | 59.3 | 6.8 | 24.8 | 52.5 | 64.3 | 5.0 |
| AW-G-Tikh-CCA+VGG+ HKSE (lin,lin) (Mean Vec) | 22.40 | 49.94 | 62.62 | 6.0 | 30.56 | 58.43 | 69.96 | 4.0 |
| AW-G-Tikh-CCA+VGG+HKSE (rbf,rbf) | 25.80 | 54.72 | 66.52 | 4.0 | 32.5 | 61.03 | 73.23 | 3.0 |
| AW-G-Tikh-CCA+VGG+[HKSE (lin,rbf)∥HKSE(rbf,rbf)] | 26.43 | 55.03 | 66.39 | 4.0 | 33.73 | 63.33 | 75.17 | 3.0 |
| AW-G-Tikh-CCA+ResNet+HKSE (lin,lin) | 28.29 | 56.81 | 69.0 | 4.0 | 37.0 | 66.67 | 78.23 | 2.0 |
| AW-G-Tikh-CCA+ResNet+[HKSE (lin,rbf)∥HKSE(rbf,rbf)] | 31.48 | 60.71 | 72.09 | 3.0 | 43.83 | 71.87 | 81.87 | 2.0 |
| AW-G-Tikhonov-CCA +VGG+ Skip thoughts | 22.18 | 48.9 | 60.92 | 6.0 | 28.23 | 56.50 | 68.36 | 4.0 |
| BRNN+VGG [1] | 15.2 | 37.7 | 50.5 | 9.2 | 22.2 | 48.2 | 61.4 | 4.8 |
| CCA+VGG+ Fisher GMM+HGLMM[5] | 25.0 | 52.7 | 66.0 | 5.0 | 35.0 | 62.0 | 73.80 | 3.0 |
| Flickr 8K | | | | | | | | |
| CCA + VGG+Mean Vec [5] | 19.1 | 45.3 | 60.4 | 7.0 | 22.6 | 48.8 | 61.2 | 6.0 |
| AW-G-Tikh-CCA+VGG+HKSE (lin,lin) (Mean Vec) | 18.62 | 44.82 | 58.88 | 7.0 | 23.10 | 50.8 | 63.00 | 5.0 |
| AW-G-Tikh-CCA+ VGG+HKSE (rbf,rbf) | 19.6 | 45.66 | 58.00 | 7.0 | 25.5 | 53.4 | 67.60 | 5.0 |
| AW-G-Tikh-CCA+VGG+[HKSE (lin,rbf)∥HKSE(rbf,rbf)] | 19.36 | 45.34 | 57.08 | 7.0 | 26.0 | 52.3 | 67.1 | 5.0 |
| AW-G-Tikh-CCA+ResNet+HKSE (lin,lin) | 23.08 | 52.18 | 65.5 | 5.0 | 32.8 | 63.4 | 74.8 | 3.0 |
| AW-G-Tikh-CCA+ResNet+[HKSE (lin,rbf)∥HKSE(rbf,rbf)] | 23.74 | 52.48 | 65.72 | 5.0 | 34.6 | 65.7 | 75.7 | 3.0 |
| AW-G-Tikhonov-CCA+VGG+Skip thoughts | 17.52 | 43.76 | 57.92 | 7.0 | 21.70 | 50.20 | 63.70 | 5.0 |
| BRNN+VGG [1] | 11.8 | 32.1 | 44.7 | 12.4 | 16.5 | 40.6 | 54.2 | 7.6 |
| CCA+VGG+Fisher GMM+HGLMM [5] | 21.2 | 50.0 | 64.8 | 5.0 | 31.0 | 59.3 | 73.7 | 4.0 |

Table 6: Mean results of the test splits on the Flickr 30 K and 8K benchmarks (in %).

allows for a better model selection and hence contributes also in improving the retrieval performance. Finally we presented the Hierarchical Kernel Sentence Embedding that is of inde-

pendent interest, and that generalizes the mean word2vec as a mean for aggregation of word embeddings and outperforms off the shelf sentence embeddings in bidirectional retrieval.

References

- [1] Andrej Karpathy and Fei-Fei Li. Deep visual-semantic alignments for generating image descriptions. In *CVPR*, 2015. 1, 8, 16
- [2] Junhua Mao, Wei Xu, Yi Yang, Jiang Wang, and Alan L. Yuille. Explain images with multimodal recurrent neural networks. *ArXiv*, 2014. 1
- [3] Oriol Vinyals, Alexander Toshev, Samy Bengio, and Dumitru Erhan. Show and tell: A neural image caption generator. *CVPR*, 2014. 1
- [4] H. Fang, S. Gupta, F. N. Iandola, R.K. Srivastava, L. Deng, P. Dollár, J. Gao, X. He, Margaret. Mitchell, J. C. Platt, C. L. Zitnick, and G. Zweig. From captions to visual concepts and back. In *CVPR*, 2015. 1
- [5] Benjamin Klein, Guy Lev, Gil Sadeh, and Lior Wolf. Associating neural word embeddings with deep image representations using fisher vectors. In *CVPR*, 2015. 1, 3, 5, 6, 7, 8, 16
- [6] Ryan Kiros, Yukun Zhu, Ruslan Salakhutdinov, Richard S. Zemel, Antonio Torralba, Raquel Urtasun, and Sanja Fidler. Skip-thought vectors. *NIPS*, 2015. 1, 6, 8
- [7] Y. Gong, L. Wang, M. Hodosh, J. Hockenmaier, and S. Lazebnik. Improving image-sentence embeddings using large weakly annotated photo collections. In *ECCV*, 2014. 1, 2, 3, 5, 6, 7
- [8] Richard Socher, Milind Ganjoo, Hamsa Sridhar, Osbert Bastani, Christopher D. Manning, and Andrew Y. Ng. Zero-shot learning through cross-modal transfer. *NIPS*, 2013. 1
- [9] H.D. Vinod. Canonical ridge and econometrics of joint production. *Journal of Econometrics*, 1976. 1, 3
- [10] Gene H. Golub, He Bjlirck, and Gene H. Golub. Numerical methods for computing angles between linear subspaces. *Math. Comp.*, 1973. 1, 3
- [11] Per C. Hansen. The truncated svd as a method for regularization. *Technical report*, 1986. 1
- [12] Tsung-Yi Lin, Michael Maire, Serge J. Belongie, Lubomir D. Bourdev, Ross B. Girshick, James Hays, Pietro Perona, Deva Ramanan, Piotr Dollár, and C. Lawrence Zitnick. Microsoft COCO: common objects in context. *ECCV*, 2014. 1, 6
- [13] Micah Hodosh, Peter Young, and Julia Hockenmaier. Framing image description as a ranking task: Data, models and evaluation metrics. *J. Artif. Int. Res.*, 2013. 1, 6, 16
- [14] Peter Young, Alice Lai, Micah Hodosh, and Julia Hockenmaier. From image descriptions to visual denotations: New similarity metrics for semantic inference over event descriptions. *TACL*, 2014. 1, 6, 16
- [15] Harold Hotelling. Relations between two sets of variates. *Biometrika*, 1936. 2
- [16] Gene H. Golub and Hongyuan Zha. Springer, 1995. 2
- [17] John Lafferty and ChengXiang Zhai. *Language Modeling for Information Retrieval*. Springer Netherlands, 2003. 2, 3, 7, 10
- [18] Tomas Mikolov, Kai Chen, Greg Corrado, and Jeffrey Dean. Efficient estimation of word representations in vector space. *ArXiv*, 2013. 5
- [19] Alex Smola, Arthur Gretton, Le Song, and Bernhard Schölkopf. A hilbert space embedding for distributions. Springer, 2007. 5
- [20] Yuya Yoshikawa, Tomoharu Iwata, Hiroshi Sawada, and Takeshi Yamada. Cross-domain matching for bag-of-words data via kernel embeddings of latent distributions. In *NIPS*. 2015. 5
- [21] Andreas Christmann and Ingo Steinwart. Universal kernels on non-standard input spaces. In *NIPS*. 2010. 5, 16
- [22] Ali Rahimi and Benjamin Recht. Random features for large-scale kernel machines. In *NIPS*. 2008. 5
- [23] Karen Simonyan and Andrew Zisserman. Very deep convolutional networks for large-scale image recognition. *ICLR*, 2015. 6
- [24] Ivan Vendrov, Ryan Kiros, Sanja Fidler, and Raquel Urtasun. Order-embeddings of images and language. *ICLR*, 2015. 6, 7, 8
- [25] Liwei Wang, Yin Li, and Svetlana Lazebnik. Learning deep structure-preserving image-text embeddings. *CVPR*, 2016. 6
- [26] Kaiming He, Xiangyu Zhang, Shaoqing Ren, and Jian Sun. Deep residual learning for image recognition. In *CVPR*, 2016. 6
- [27] Luke Vilnis and Andrew McCallum. Word representations via gaussian embedding. *ICLR*, 2015. 16
- [28] Tony Jebara and Risi Kondor. Bhattacharyya and expected likelihood kernels. In *COLT*, 2003. 16

Supplementary Material

Asymmetric Regularized CCA and Hierarchical Kernel Sentence Embedding for Image & Text Retrieval

A. Appendix: Query Generation Versus Search Generation

[17] propose to use a binary random variable r that denotes relevance between a query and a search item, $r = 1$ if there is a match and 0 otherwise. In order to rank search items [17] propose the use of the log-odds ratio:

$$\log \frac{\mathbb{P}(r = 1|q, s)}{\mathbb{P}(r = 0|q, s)}$$

Using the search generation approach this ratio is equivalent to [17]:

$$\log \frac{\mathbb{P}(s|q, r = 1)}{\mathbb{P}(s|q, r = 0)},$$

hence this approach needs both positive and negative pairs of search and query items (triplet losses are instances of this approach). On the other hand using the query generation approach (under mild assumptions) this ratio is equivalent to [17]:

$$\log \mathbb{P}(q|s, r = 1)$$

The query generation approach models relevance in an implicit way and does not need negative samples.

B. Appendix: Proofs

Proof 1 (Proof of Lemma 1) We give the proof here as it will be useful in the the development of the full regularization path of CCA with truncated SVD regularization of the covariances C_{XX} and C_{YY} . Let $P_x = \Sigma_x V_x^\top U \in \mathbb{R}^{m_x \times k}$ equivalently $U = V_x \Sigma_x^{-1} P_x$ and $P_y = \Sigma_y V_y^\top V \in \mathbb{R}^{m_y \times k}$ equivalently $V = V_y \Sigma_y^{-1} P_y$. Hence we obtain by this change of variable: $U^\top X^\top Y V = P_x^\top \Sigma_x^{-1} V_x^\top V_x \Sigma_x U^\top U_y \Sigma_y V_y^\top V_y \Sigma_y^{-1} P_y = P_x^\top (U_x^\top U_y) P_y$. Similarly: $U^\top X^\top X U = P_x^\top P_x$ $V^\top Y^\top Y V = P_y^\top P_y$. Hence replacing U, V with P_x, P_y we have:

$$\max_{P_x^\top P_x = I, P_y^\top P_y = I} \text{Tr}(P_x^\top (U_x^\top U_y) P_y),$$

This is solved by an SVD of $T = U_x^\top U_y$. $[P_x, \Sigma, P_y] = \text{SVD}(T)$, ($P_x \in \mathbb{R}^{m_x \times k}, \Sigma \in \mathbb{R}^{k \times k}, P_y \in \mathbb{R}^{m_y \times k}$). where $k = \min(m_x, m_y)$, and finally we have $U = V_x \Sigma_x^{-1} P_x$, $V = V_y \Sigma_y^{-1} P_y$.

Proof 2 (Proof of Theorem 1)

1) Tikhonov:

$$\max_{U^\top (X^\top X + \gamma_x I) U = I, V^\top (Y^\top Y + \gamma_y I) V = I} \text{Tr}(U^\top X^\top Y V). \quad (10)$$

$[U_x, \Sigma_x, V_x] = \text{SVD}(X)$ $U_x \in \mathbb{R}^{n \times m_x}, \Sigma_x \in \mathbb{R}^{m_x \times m_x}, V_x \in \mathbb{R}^{m_x \times m_x}$ $X = U_x \Sigma_x V_x^\top$. $[U_y, \Sigma_y, V_y] = \text{SVD}(Y)$ $U_y \in \mathbb{R}^{n \times m_y}, \Sigma_y \in \mathbb{R}^{m_y \times m_y}, V_y \in \mathbb{R}^{m_y \times m_y}$ $Y = U_y \Sigma_y V_y^\top$.

$$X^\top X + \gamma_x I = V_x (\Sigma_x^2 + \gamma_x I) V_x^\top.$$

$$Y^\top Y + \gamma_y I = V_y (\Sigma_y^2 + \gamma_y I) V_y^\top.$$

Let $P_x = \sqrt{\Sigma_x^2 + \gamma_x I} V_x^\top U \in \mathbb{R}^{m_x \times k}$ equivalently $U = V_x (\Sigma_x^2 + \gamma_x I)^{-\frac{1}{2}} P_x$. Let $P_y = \sqrt{\Sigma_y^2 + \gamma_y I} V_y^\top V \in \mathbb{R}^{m_y \times k}$ equivalently $V = V_y (\Sigma_y^2 + \gamma_y I)^{-\frac{1}{2}} P_y$. Hence we obtain by this change of variable for the objective in (10):

$$\begin{aligned} U^\top X^\top Y V &= P_x^\top (\Sigma_x^2 + \gamma_x I)^{-\frac{1}{2}} V_x^\top V_x \Sigma_x U^\top U_y \Sigma_y V_y^\top V_y (\Sigma_y^2 + \gamma_y I)^{-\frac{1}{2}} P_y \\ &= P_x^\top (\Sigma_x^2 + \gamma_x I)^{-\frac{1}{2}} \Sigma_x (U_x^\top U_y) \Sigma_y (\Sigma_y^2 + \gamma_y I)^{-\frac{1}{2}} P_y. \end{aligned}$$

Let

$$T_{\gamma_x, \gamma_y} = (\Sigma_x^2 + \gamma_x I)^{-\frac{1}{2}} \Sigma_x (U_x^\top U_y) \Sigma_y (\Sigma_y^2 + \gamma_y I)^{-\frac{1}{2}},$$

hence we have:

$$U^\top X^\top Y V = P_x^\top T_{\gamma_x, \gamma_y} P_y.$$

On the other hand, plugging this change of variable in the constraints of (10) we obtain:

$$U^\top (X^\top X + \gamma_x I) U = U^\top V_x (\Sigma_x^2 + \gamma_x I) V_x^\top U = P_x^\top P_x = I$$

$$V^\top (Y^\top Y + \gamma_y I) V = V^\top V_y (\Sigma_y^2 + \gamma_y I) V_y^\top V = P_y^\top P_y = I$$

Therefore using this change of variable, problem (10) becomes:

$$\max_{P_x^\top P_x = I, P_y^\top P_y = I} Tr(P_x^\top T_{\gamma_x, \gamma_y} P_y), \quad (11)$$

this is the variational formulation of the SVD of T_{γ_x, γ_y} . Hence we obtain that:

$$[P_x, \Sigma, P_y] = SVD(T_{\gamma_x, \gamma_y}),$$

$$U = V_x (\Sigma_x^2 + \gamma_x I)^{-\frac{1}{2}} P_x,$$

$$V = V_y (\Sigma_y^2 + \gamma_y I)^{-\frac{1}{2}} P_y.$$

2) T-SVD:

$$\max_{U^\top X_{k_x}^\top X_{k_x} U = I, V^\top Y_{k_y}^\top Y_{k_y} V = I} Tr(U^\top X^\top Y V) \quad (12)$$

Let

$$P_x = \Sigma_{k_x} V_{k_x}^\top U \in \mathbb{R}^{k_x \times k}, \quad \text{equivalently } U = V_{k_x} \Sigma_{k_x}^{-1} P_x \in \mathbb{R}^{m_x \times k}, k = \min(k_x, k_y)$$

$$P_y = \Sigma_{k_y} V_{k_y}^\top V \in \mathbb{R}^{k_y \times k}, \quad \text{equivalently } V = V_{k_y} \Sigma_{k_y}^{-1} P_y \in \mathbb{R}^{m_y \times k}, k = \min(k_x, k_y)$$

Hence we obtain by this change of variable, in the objective of (12):

$$U^\top X^\top Y V = P_x^\top \Sigma_{k_x}^{-1} V_{k_x}^\top V_x \Sigma_x U_x^\top U_y \Sigma_y V_y^\top V_{k_y} \Sigma_{k_y}^{-1} P_y,$$

Now we turn to:

$$\begin{aligned} \Sigma_{k_x}^{-1} (V_{k_x}^\top V_x) \Sigma_x U_x^\top &= \Sigma_{k_x}^{-1} [I_{k_x \times k_x} \ 0_{k_x \times (m_x - k_x)}] \Sigma_x U_x^\top \\ &= \Sigma_{k_x}^{-1} [\Sigma_{k_x} \ 0_{k_x \times (m_x - k_x)}] U_x^\top \\ &= [I_{k_x \times k_x} \ 0_{k_x \times (m_x - k_x)}] U_x^\top \\ &= U_{k_x}^\top \end{aligned}$$

Hence we keep the first k_x columns of U_x , that is U_{k_x} . The same argument hold for U_{k_y} . It follows that using truncated SVD, we have:

$$U^\top X^\top Y V = P_x^\top U_{k_x}^\top U_{k_y} P_y.$$

Let

$$T_{k_x, k_y} = U_{k_x}^\top U_{k_y},$$

then using this change of variable, the objective in (12) becomes:

$$U^\top X^\top Y V = P_x^\top T_{k_x, k_y} P_y.$$

Now turning to the constraints of (12), using this change of variable we obtain:

$$U^\top X_{k_x}^\top X_{k_x} U = U^\top V_{k_x} \Sigma_{k_x}^2 V_x^\top U = P_x^\top P_x = I,$$

$$V^\top Y_{k_y}^\top Y_{k_y} V = V^\top V_{k_y} \Sigma_{k_y}^2 V_y^\top V = P_y^\top P_y = I.$$

Therefore using this change of variable, problem (12) becomes:

$$\max_{P_x^\top P_x = I, P_y^\top P_y = I} Tr(P_x^\top T_{k_x, k_y} P_y), \quad (13)$$

this is the variational formulation of the SVD of T_{k_x, k_y} . Hence truncated SVD-CCA can be solved finding:

$$[P_{k_x}, \Sigma^{k_x, k_y}, P_{k_y}] = SVD(T_{k_x, k_y}).$$

Turning now to $U_{k_x}^\top U_{k_y}$ this can be computed efficiently by precomputing $T = U_x^\top U_y \in \mathbb{R}^{m_x \times m_y}$ and then extracting the submatrix consisting of k_x rows and k_y columns. we return therefore $U = V_{k_x} \Sigma_{k_x}^{-1} P_x$, $V = V_{k_y} \Sigma_{k_y}^{-1} P_y$.

C. Algorithms

Algorithm 1 Bjorck Golub

- 1: $[U_x, \Sigma_x, V_x] = SVD(X)$.
 - 2: $[U_y, \Sigma_y, V_y] = SVD(Y)$.
 - 3: $T = U_x^\top U_y \in \mathbb{R}^{m_x \times m_y}$
 - 4: $[P_x, \Sigma, P_y] = SVD(T)$
 - 5: $U = V_x \Sigma_x^{-1} P_x$
 - 6: $V = V_y \Sigma_y^{-1} P_y$
 - 7: return U, V
-

Algorithm 2 Tikhonov Regularized CCA (X, Y)

- 1: $[U_x, \Sigma_x, V_x] = SVD(X)$.
 - 2: $[U_y, \Sigma_y, V_y] = SVD(Y)$.
 - 3: $T_0 = \Sigma_x (U_x^\top U_y) \Sigma_y \in \mathbb{R}^{m_x \times m_y}$
 - 4: **for** $\gamma_x \in \{\sigma_{x,1}^2, \dots, \sigma_{x,m_x}^2\}$ **do**
 - 5: ▷ The set of singular values squared or a subsampled grid
 - 6: **for** $\gamma_y \in \{\sigma_{y,1}^2, \dots, \sigma_{y,m_y}^2\}$ **do**
 - 7: $T = (\Sigma_x^2 + \gamma_x I)^{-\frac{1}{2}} T_0 (\Sigma_y^2 + \gamma_y I)^{-\frac{1}{2}}$
 - 8: $[P_x, \Sigma^{\gamma_x, \gamma_y}, P_y] = SVD(T)$
 - 9: $U = V_x (\Sigma_x^2 + \gamma_x I)^{-\frac{1}{2}} P_x$
 - 10: $V = V_y (\Sigma_y^2 + \gamma_y I)^{-\frac{1}{2}} P_y$
 - 11: Compute performance using $U, V, \Sigma^{\gamma_x, \gamma_y}$ on a validation Set.
 - 12: (Bidirectional Retrieval is done using a sorted list of the scores of AW-CCA)
 - 13: **end for**
 - 14: **end for**
 - 15: return $U, V, \Sigma^{\gamma_x, \gamma_y}, \gamma_x, \gamma_y$ with best validation performance for each task.
-

Algorithm 3 Truncated SVD CCA (X,Y)

- 1: $[U_x, \Sigma_x, V_x] = SVD(X)$.
 - 2: $[U_y, \Sigma_y, V_y] = SVD(Y)$.
 - 3: $T = U_x^\top U_y \in \mathbb{R}^{m_x \times m_y}$
 - 4: $W^x = V_x \Sigma_x^{-1} \in \mathbb{R}^{m_x \times m_x}$
 - 5: $W^y = V_y \Sigma_y^{-1} \in \mathbb{R}^{m_y \times m_y}$
 - 6: **for** $k_x \in [m_x]$ **do** $\triangleright [m_x] = \{1 \dots m_x\}$ or a subsampled grid.
 - 7:
 - 8: **for** $k_y \in [m_y]$ **do**
 - 9: $[P_x, \Sigma^{k_x, k_y}, P_y] = SVD(T_{1:k_x, 1:k_y})$ $\triangleright T_{1:k_x, 1:k_y}$: extracts the first k_x rows ,and the first k_y columns of T .
 - 10:
 - 11: $U = W^x_{:, 1:k_x} P_x$
 - 12: $V = W^y_{:, 1:k_y} P_y$
 - 13: Compute performance using U, V, Σ^{k_x, k_y} on a validation Set.
 - 14: (Bidirectional Retrieval is done using a sorted list of the scores of AW-CCA.)
 - 15: **end for**
 - 16: **end for**
 - 17: return $U, V, \Sigma^{k_x, k_y}, k_x, k_y$ with best validation performance for each task.
-

Algorithm 4 Guided Tikhonov Validation by T-SVD(X,Y)

- 1: $(k_x^*, k_y^*) = \text{Truncated SVD CCA}(X, Y)$
 - 2: $(\gamma_x, \gamma_y) = (\sigma_{x, k_x^*}^2, \sigma_{y, k_y^*}^2)$
 - 3: $[P_x, \Sigma^{\gamma_x, \gamma_y}, P_y] = SVD(T_{\gamma_x, \gamma_y})$
 - 4: $U = V_x (\Sigma_x^2 + \gamma_x I)^{-\frac{1}{2}} P_x$,
 - 5: $V = V_y (\Sigma_y^2 + \gamma_y I)^{-\frac{1}{2}} P_y$
 - 6: return $U, V, \Sigma^{\gamma_x, \gamma_y}$.
-

D. Query Generation versus Search Generation versus CCA

When we retrieve images matching a text query. Three methods are possible:

1. CCA: We cross validate from image search using the cosine $\frac{\langle U^\top x, V^\top y \rangle}{\|U^\top x\| \|V^\top y\|}$. Then we retrieve for the test query images with largest cosine.
2. Query Generation Approach: Where we weigh the canonical weights of search space (images) that is U , we cross-validate using the score $\frac{\langle \Sigma U^\top x, V^\top y \rangle}{\|\Sigma U^\top x\| \|V^\top y\|}$. We retrieve for the query y images having largest score as defined here.
3. Search Generation Approach: Where we weigh the canonical weights of query space (text) that is V , we cross-validate using the score $\frac{\langle U^\top x, \Sigma V^\top y \rangle}{\|U^\top x\| \|\Sigma V^\top y\|}$

To illustrate this we consider the following text query:" A kitchen with two windows and two metals sinks". We embed this sentence using HKSE(rbf,rbf) get a vector y . We do three experiments:

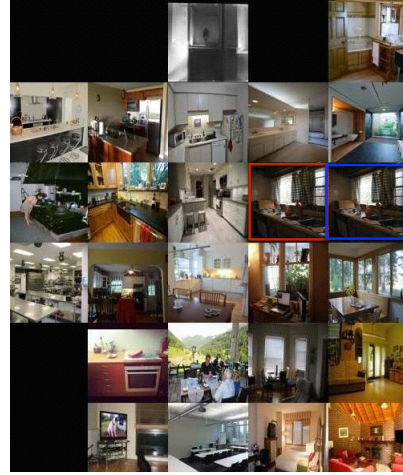
1. We embed the image test set with ΣU^\top , and the query with V^\top , this corresponds to the Query generation approach. Then we embed the query and the nearest neighbor images in 2D using the t-SNE plot. We represent the text query with the ground truth image with a blue box around it.
2. We embed the image test set with U^\top , and the query with V^\top , this corresponds to CCA. Then we embed the query and the nearest neighbor images in 2D using the t-SNE plot. We represent the text query with the ground truth image with a blue box around it.

3. We embed the image test set with U^\top , and the query with ΣV^\top , this corresponds to the search generation approach. Then we embed the query and the nearest neighbor images in 2D using the t-SNE plot. We represent the text query with the ground truth image with a blue box around it.

We see in Figure 3 that the space is better organized in the query generation approach.

Text Query: A kitchen with two windows and two metal sinks

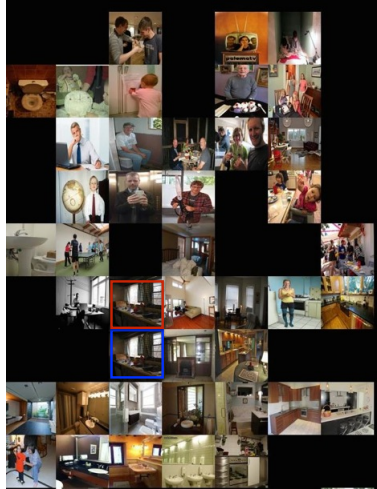
Ground Truth Image:



$$\left(\underbrace{\Sigma U^\top x}_{\text{Search item}}, \underbrace{V^\top y}_{\text{Query item}} \right)$$

$$S \rightarrow Q$$

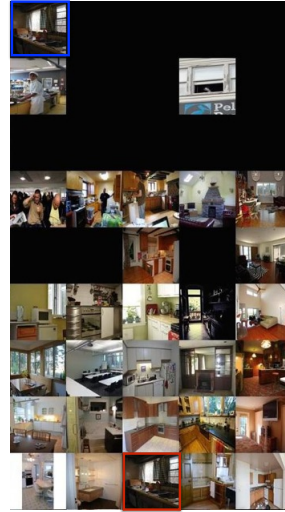
(a) Query Generation Approach.



$$\left(\underbrace{U^\top x}_{\text{Search item}}, \underbrace{V^\top y}_{\text{Query item}} \right)$$

$$S \rightarrow Z \leftarrow Q$$

(b) CCA.



$$\left(\underbrace{U^\top x}_{\text{Search item}}, \underbrace{\Sigma V^\top y}_{\text{Query item}} \right)$$

$$Q \rightarrow S$$

(c) Search Generation Approach.

Figure 3: TSNE plots of different Embeddings.

E. HKSE

E.1. Proof of Proposition 1

Proposition 2 (HKSE approximation) Let \mathcal{A} be the vocabulary embedded in a vector space. Let $|\mathcal{A}|$ be the size of the vocabulary. Let s be the maximum sentence length. Let $\hat{\mu}_{n_1}(\rho_1) = \frac{1}{n_1} \sum_{i=1}^{n_1} \Phi_{\gamma,d}(a_i)$, and $\hat{\mu}_{n_2}(\rho_2) = \frac{1}{n_2} \sum_{i=1}^{n_2} \Phi_{\gamma,d}(b_i)$, on two different sentences ρ_1, ρ_2 , with words $\{a_1, \dots, a_{n_1}\}$ and $\{b_1, \dots, b_{n_2}\}$ respectively. Let $\epsilon, \delta > 0$, for $m \geq \frac{1}{2\delta^2} \log(|\mathcal{A}|^2/\epsilon)$

and $m' \geq \frac{1}{2\delta^2} \log(|\mathcal{A}|^{2s}/\epsilon)$ we have with probability $1 - 2\epsilon$:

$$\exp \frac{-3\eta\delta}{2} K(\rho_1, \rho_2) - \delta \leq \langle \Phi_{\eta, m}(\hat{\mu}_{n_1}(\rho_1)), \Phi_{\eta, m}(\hat{\mu}_{n_2}(\rho_2)) \rangle \leq \exp \frac{3\eta\delta}{2} K(\rho_1, \rho_2) + \delta,$$

Informally for 2 layers the error of estimation is multiplicative and additive, inner word level dimension scales logarithmically with the vocabulary size $m = O(\log(|\mathcal{A}|))$, and the outer dimension scales linearly with the maximum sentence length s and logarithmically with the vocabulary size $m' = O(s \log(|\mathcal{A}|))$.

Proof 3 Let \mathcal{A} be the vocabulary embedded in a vector space. Let $|\mathcal{A}|$ be the size of the vocabulary. We know from Rahimi and Rech that :

$$\mathbb{E} \langle \Phi_{\gamma, d}(a), \Phi_{\gamma, d}(b) \rangle = k_{\gamma, d}(a, b) \text{ for all } a, b \in \mathcal{A}$$

Hence applying Hoeffding inequality and a union bound on all words in \mathcal{A} , we obtain that, the following holds with a probability $1 - \epsilon$ for all $a, b \in \mathcal{A}$:

$$k_{\gamma, d}(a, b) - \delta \leq \langle \Phi_{\gamma, d}(a), \Phi_{\gamma, d}(b) \rangle \leq k_{\gamma, d}(a, b) + \delta,$$

for $m \geq \frac{1}{2\delta^2} \log(|\mathcal{A}|^2/\epsilon)$.

Let $\hat{\mu}_{n_1}(\rho_1) = \frac{1}{n_1} \sum_{i=1}^{n_1} \Phi_{\gamma, d}(a_i)$, and $\hat{\mu}_{n_2}(\rho_2) = \frac{1}{n_2} \sum_{i=1}^{n_2} \Phi_{\gamma, d}(b_i)$, on two different sentences. Assume s is the maximum sentence length, a bound on the total number of sentence is $|\mathcal{A}|^s$. Applying again a hoeffding bound, and a union bound on all sentences, we have with a probability $1 - \epsilon$

$$k_{\eta, m}(\hat{\mu}_{n_1}(\rho_1), \hat{\mu}_{n_2}(\rho_2)) - \delta \leq \langle \Phi_{\eta, m}(\hat{\mu}_{n_1}(\rho_1)), \Phi_{\eta, m}(\hat{\mu}_{n_2}(\rho_2)) \rangle \leq k_{\eta, m}(\hat{\mu}_{n_1}(\rho_1), \hat{\mu}_{n_2}(\rho_2)) + \delta,$$

for $m' \geq \frac{1}{2\delta^2} \log(|\mathcal{A}|^{2s}/\epsilon)$. Let $\Delta = \frac{1}{n_1^2} \sum_{i, j=1}^{n_1} k_{\gamma, d}(a_i, a_j) + \frac{1}{n_2^2} \sum_{i, j=1}^{n_2} k_{\gamma, d}(b_i, b_j) - \frac{1}{n_1 n_2} \sum_{i=1}^{n_1} \sum_{j=1}^{n_2} 2k_{\gamma, d}(a_i, b_j)$. By definition:

$$K(\rho_1, \rho_2) = \exp\left(-\frac{\eta}{2} \Delta\right)$$

$$\begin{aligned} k_{\eta, m}(\hat{\mu}_{n_1}(\rho_1), \hat{\mu}_{n_2}(\rho_2)) &= \exp -\frac{\eta}{2} \left(\|\hat{\mu}_{n_1}(\rho_1) - \hat{\mu}_{n_2}(\rho_2)\|_2^2 \right) \\ &= \exp -\frac{\eta}{2} \left(\|\hat{\mu}_{n_1}(\rho_1) - \hat{\mu}_{n_2}(\rho_2)\|_2^2 - \Delta + \Delta \right) \\ &= K(\rho_1, \rho_2) \exp -\frac{\eta}{2} \left(\|\hat{\mu}_{n_1}(\rho_1) - \hat{\mu}_{n_2}(\rho_2)\|_2^2 - \Delta \right) \end{aligned}$$

Note that $m \geq \frac{1}{2\delta^2} \log(|\mathcal{A}|^2/\epsilon)$, we have with probability $1 - \epsilon$,

$$\left| \|\hat{\mu}_{n_1}(\rho_1) - \hat{\mu}_{n_2}(\rho_2)\|_2^2 - \Delta \right| \leq 3\delta$$

Hence with probability $1 - \epsilon$

$$\exp \frac{-3\eta\delta}{2} K(\rho_1, \rho_2) \leq k_{\eta, m}(\hat{\mu}_{n_1}(\rho_1), \hat{\mu}_{n_2}(\rho_2)) \leq \exp \frac{3\eta\delta}{2} K(\rho_1, \rho_2)$$

Hence for $m \geq \frac{1}{2\delta^2} \log(|\mathcal{A}|^2/\epsilon)$ and $m' \geq \frac{1}{2\delta^2} \log(|\mathcal{A}|^{2s}/\epsilon)$ we have with probability $1 - 2\epsilon$:

$$\exp \frac{-3\eta\delta}{2} K(\rho_1, \rho_2) - \delta \leq \langle \Phi_{\eta, m}(\hat{\mu}_{n_1}(\rho_1)), \Phi_{\eta, m}(\hat{\mu}_{n_2}(\rho_2)) \rangle \leq \exp \frac{3\eta\delta}{2} K(\rho_1, \rho_2) + \delta,$$

Informally for 2 layers the error of estimation is multiplicative and additive, the inner word level dimension scales logarithmically with the vocabulary size $m = O(\log(|\mathcal{A}|))$, and the outer dimension scales linearly with the maximum sentence length s and logarithmically with the vocabulary size $m' = O(s \log(|\mathcal{A}|))$.

E.2. HKSE as a Gaussian Embedding of Sentences

[27] introduced the embedding of words to Gaussian distributions (Word2Gauss), we show that similarly HKSE(lin,rbf) for k^w being linear and k^s being an rbf (radial basis function) kernel defines an embedding of sentences to Gaussian distributions (Sent2Gauss). Given $\{a_1 \dots a_n\}$, the vector embeddings of words in a sentence, we represent a sentence as a gaussian distribution $\rho : \rho \sim \mathcal{N}(\mu, \sigma^2 I_d)$, $\mu = \frac{1}{n} \sum_{i=1}^n a_i, \eta > 0$. In order to compare two sentences we compare two distributions ρ_1 and ρ_2 , using product kernel between distributions [28]: $K(\rho_1, \rho_2) = \int \mathcal{N}(x; \mu_1, \sigma^2 I_d) \mathcal{N}(x; \mu_2, \sigma^2 I_d) dx = \mathcal{N}(0; \mu_1 - \mu_2, 2\sigma^2 I_d) = (4\pi\sigma^2)^{-\frac{d}{2}} \exp\left(-\frac{1}{4\sigma^2} \|\mu_1 - \mu_2\|^2\right)$, which corresponds to the kernel computed by HKSE(lin,rbf). HKSE(rbf,rbf) corresponds also to a universal kernel between distributions [21].

F. Data Splits

For MSCOCO the training set contains 113,287 images, along with 5 captions each. Similarly to [5], we used the splits from [1], and performed cross-validation on a validation set of 5K images, and tested our models on a test set of 5K images, as well as five 1K splits of the 5K test images as in [5]. We report for both tasks the recall rate at one result, five results, or ten first results (r@1,5,10), as well as the median rank of the first ground truth retrieval.

We follow the experimental protocol of github.com/ryankiros/skip-thoughts/blob/master/eval_rank.py: For 5K test images, we have 25K query captions, the image search retrieval scoring is based on the ground truth image of each caption. For image annotation, we have 5K query test images, to annotate among 25K captions, the scoring returns the caption that has the highest cosine within each 5 captions. A similar scoring is done for 1K tests. We did not do any vocabulary pruning and kept all words that in vocabulary of word2vec we ended up with a vocabulary size 21975 words for MSCOCO.

The Flickr 8K training set contains 6K images along with 5 captions each, the validation and test set contain 1K images each. We use the splits as specified in [13]. The Flickr 30K [14] training set contains 25381 images along with 5 captions each, the validation and test sets contain 3K images each. We follow [1] and use 3 random splits of 1K images for test and validation and report average performance over three runs. We did not do any vocabulary pruning and kept all words that in vocabulary of word2vec we ended up with a vocabulary size 16772 words for Flickr30 K and 7745 for Flickr 8k.

G. AWT-SVD CCA Regularization Paths

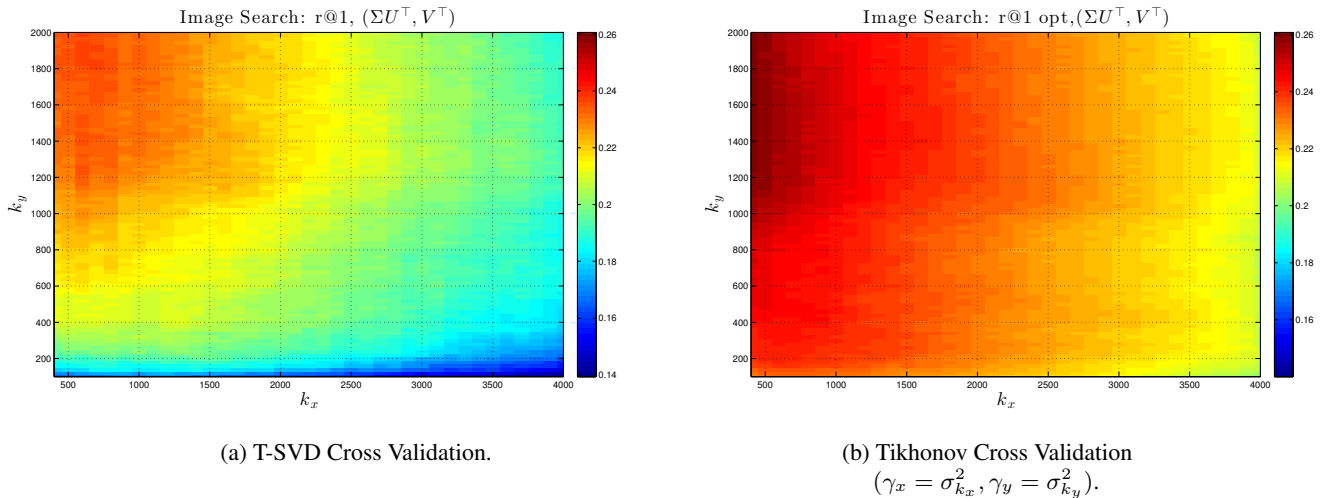
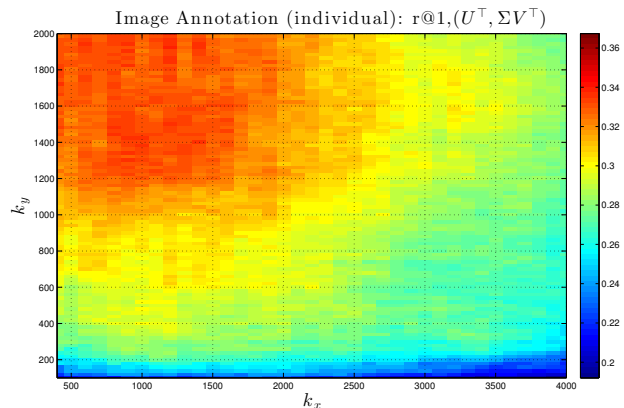
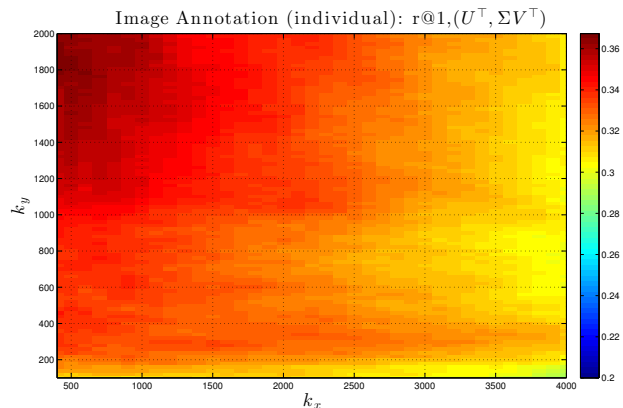


Figure 4: Regularization Path for T-SVD CCA, and Tikhonov CCA on bidirectional retrieval on Flickr30K with VGG features (4096 dimensions) for the image and HKSE(rbf,rbf) (2000 dimensions). Cross validation was performed on the validation set on grid going from 400 to 4000 with step size of 100 for k_x , and from 200 to 2000 with a step size of 20 for k_y . We report r@1 of the retrieved query over the validation set (Higher is better, in red). We see that T-SVD and Tikhonov select the same region of interest, justifying the T-SVD guided Tikhonov approach.

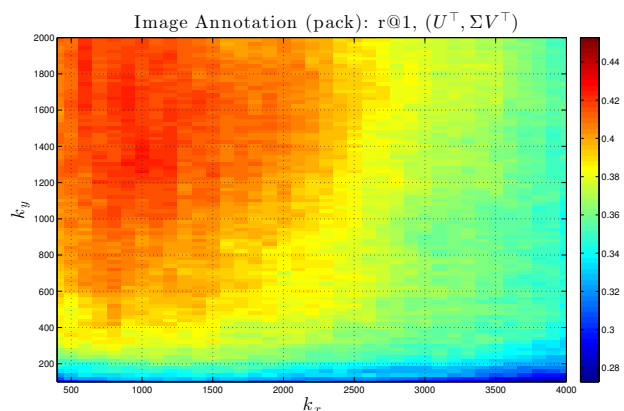


(a) T-SVD Cross Validation.

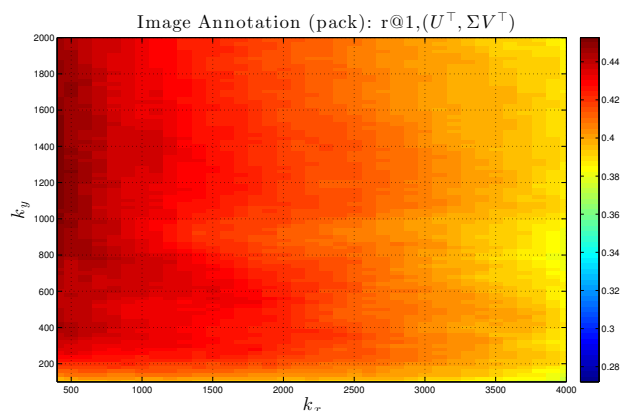


(b) Tikhonov Cross Validation
 $(\gamma_x = \sigma_{k_x}^2, \gamma_y = \sigma_{k_y}^2)$.

Figure 5: Regularization Path for T-SVD CCA , and Tikhonov CCA on bidirectional retrieval on Flickr30K with VGG features (4096 dimensions) for the image and HKSE(rb,rbf) (2000 dimensions). Cross validation was performed on the validation set on grid going from 400 to 4000 with step size of 100 for k_x , and from 200 to 2000 with a step size of 20 for k_y . We report $r@1$ of the retrieved query over the validation set (Higher is better, in red). We see that T-SVD and Tikhonov select the same region of interest, justifying the T-SVD guided Tikhonov approach.



(a) T-SVD Cross Validation

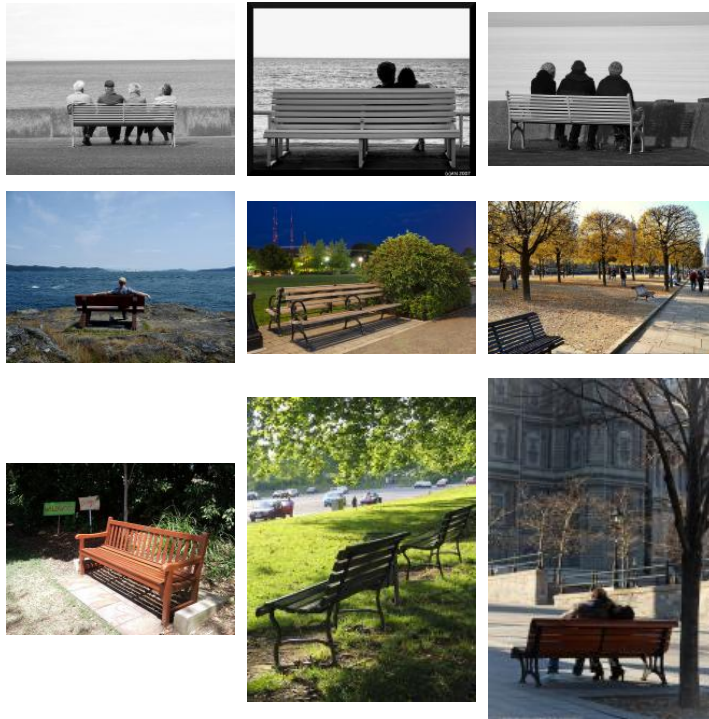


(b) Tikhonov Cross Validation
 $(\gamma_x = \sigma_{k_x}^2, \gamma_y = \sigma_{k_y}^2)$.

Figure 6: Regularization Path for T-SVD CCA , and Tikhonov CCA on bidirectional retrieval on Flickr30K with VGG features (4096 dimensions) for the image and HKSE(rb,rbf) (2000 dimensions). Cross validation was performed on the validation set on grid going from 400 to 4000 with step size of 100 for k_x , and from 200 to 2000 with a step size of 20 for k_y . We report $r@1$ of the retrieved query over the validation set (Higher is better, in red). We see that T-SVD and Tikhonov select the same region of interest, justifying the T-SVD guided Tikhonov approach.

H. Examples of Annotation and Search with AW-CCA with HKSE(rbf,rbf) and VGG

a group of four elders sit on a park bench in front of the od



a tennis ball sitting on a tennis racket



Figure 7: Image Search Results for two random text queries from COCO test set.



1. a rusty apparatus is laying in a green thicket 0.201528
2. a pile of scrap metal sitting on the floor of a forest 0.201528
3. the rusty remains of a metal device in green weeds 0.201528
4. old rusted metal on the floor with many plants and trees 0.201528
5. a pile of rusted metal junk laying in the weeds 0.201528
6. a worn wooden bench beneath some shade trees 0.171817
7. a wooden bench with metal arms is sitting outside 0.171817
8. a closeup of an old and mossy outdoor garden bench 0.171817
9. a bench is shown in the dirt by the house 0.171817
10. a worn wooden bench is sitting outside in the dirt 0.171817



1. a woman getting her hair brushed in front of other women 0.164182
2. a group of people dressed in old fashioned clothes 0.164182
3. a group of young women in costume brushing each others hair 0.164182
4. a large number of people dressed in old fashioned clothes 0.164182
5. a group of woman dressed in vintage clothing 0.164182
6. a group photo from the 1960 's of teenagers in suits and dresses 0.151239
7. a big group of people posing for a picture 0.151239
8. a black and white photograph of people at a party 0.151239
9. a group of people are gathered for a photo 0.151239
10. a black and white picture of a group of people 0.151239

Figure 8: Image Annotation results for two images outside the COCO set using Ann pack.